Regular Research Article
Short Title: Frequency response of photosynthesis
Author for Contact: Ladislav Nedbal, l.nedbal@fz-juelich.de

Photosynthesis dynamics and regulation sensed in the frequency domain

Ladislav Nedbal[1] and Dušan Lazár[2]

[1] Institute of Bio- and Geosciences/Plant Sciences (IBG-2), Forschungszentrum Jülich, Wilhelm-Johnen-Straße, D-52428 Jülich, Germany

[2] Department of Biophysics, Centre of the Region Haná for Biotechnological and Agricultural Research, Šlechtitelů 27, 783 71 Olomouc, Czech Republic

One sentence summary: It is proposed to characterize photosynthesis in the frequency domain without the need for dark adaptation and, thus, without assumptions about the dark-to-light transition.

Funding information:
L.N. gratefully acknowledges the financial support by the Federal Ministry of Education and Research of Germany (BMBF) in the framework of YESPVNIGBEN project (03SF0576A).
D.L. was supported from European Regional Development Fund project "Plants as a tool for sustainable global development" (CZ.02.1.01/0.0/0.0/16_019/0000827).

[1] L.N. conceived the study, did the experiments, analyzed the experimental data, performed the analytical calculations, wrote parts of the manuscript and was responsible for finalizing it.
[2] D.L. performed the numerical calculations, analyzed the experimental data, wrote parts of the manuscript and supervised the literature screening and referencing.

Abstract

Foundations of photosynthesis research have been established mainly by studying the response of plants to changing light, typically to sudden exposure to a constant light intensity after a dark acclimation or to light flashes. This approach remains valid and powerful, but can be limited by requiring dark acclimation prior to time-domain measurements and often assumes that rate constants determining the photosynthetic response do not change between the dark- and light-acclimation.

We present experimental data and a mathematical model demonstrating that these limits can be overcome by measuring plant responses to sinusoidally modulated light of varying frequency. By its nature, such frequency domain characterization is performed in light-acclimated plants with no need for prior dark acclimation. Amplitudes, phase shifts and upper harmonic modulation extracted from the data for a wide range of frequencies can target different kinetic domains and regulatory feedbacks. The occurrence of upper harmonic modulation reflects non-linear phenomena, including photosynthetic regulation. To support these claims, we present a frequency and time domain response in chlorophyll fluorescence emission of the green alga *Chlorella sorokiniana* in the frequency range 1000 – 0.001 Hz. Based on these experimental data and on numerical as well as analytical mathematical models, we propose that the frequency domain measurements can become a versatile new tool in plant sensing.

Introduction

The fundamental principles and structures performing oxygenic photosynthesis are highly conserved in all plants and algae. Diversity appears with adaptation and acclimation that are required for optimal performance in relevant climatic conditions, including dynamically changing light intensities and temperatures (Singsaas and Sharkey 1998, Cruz et al. 2016). Balancing linear and cyclic electron pathways among two serially operating photosystems in a dynamic environment requires elaborate regulation (Tikhonov 2015, Armbruster et al. 2017) to optimize yields and minimize potential damage by harmful by-products such as reactive oxygen species (Pospíšil 2016, Foyer 2018).

The dynamic complexity of photosynthesis is typically approached in the time-domain by studying responses that occur when dark-acclimated plants or algal cells are suddenly exposed to light. Chlorophyll (Chl) fluorescence induction that occurs upon light exposure is one of the most frequently used biophysical methods in plant physiology. The response to strong light, referred to in the literature as O-I_1-I_2-P (Neubauer and Schreiber 1987) or O-J-I-P transient (Strasser and Govindjee 1991), is very rapid, and consists of clearly discernable phases that can be analyzed using numerical deconvolution (Stirbet et al. 2018). Exposure to lower actinic light intensities common in the natural

plant environment leads to a slower induction, called the Kautsky-Hirsch effect (Govindjee 1995), that can be combined with multi-turnover saturation pulses probing photochemical and non-photochemical quenching (reviewed in Lazár 2015). The spectrum of Chl fluorescence techniques is further enlarged by methods that apply single-turnover flashes (e.g., Kolber et al. 1998, Nedbal et al. 1999). Another important set of Chl fluorescence methods exploits time resolution even further using ultrashort flashes that allow resolution of primary photosynthetic processes in reaction centers (Chukhutsina et al. 2019).

The dynamic range that needs to be considered spans more than 19 orders of magnitude, from elemental energetic processes in the reaction centers ($\approx 10^{-12}$ s), to regulation and acclimation processes that can be as slow as days ($\approx 10^{5}$ s) or seasons ($\approx 10^{7}$ s). Interpreting such a diversity of dynamic phenomena based on mathematical models is hindered by non-linear interactions that may link, e.g., slow regulation and fast primary processes. Another challenge in understanding photosynthesis dynamics is that thylakoids are far from rigid, with substantial conformational changes in photosynthetic proteins occurring already within the first seconds of exposing dark-acclimated samples to light (Schansker et al. 2011, Suga et al. 2017, Magyar et al. 2018, Oja and Laisk 2020, Sipka et al. 2021). The system dynamics during this fast phase of induction is therefore determined not only by filling the charge pools or saturating the pathways but also by the systemic thylakoid re-arrangement, all leading to potential non-linearity of the investigated system. To describe this situation, one can discriminate between the constitutive non-linearity directly related to primary photosynthetic functions and regulatory non-linearity (Bich et al., 2016). The latter is due to regulatory interactions activated by a dedicated subsystem that is dynamically decoupled from the regulated one and that is not performing constitutive functions. With this categorization, energization of the thylakoid membrane, including cyclic electron transport and saturation of photosynthetic pathways, represents constitutive non-linearity because the involved processes constitute the primary function of photosynthetic apparatus. The non-photochemical quenching (NPQ) facilitated by dedicated PsbS and violoxanthin de-epoxidase systems responding to lumen acidification is a prime example of a regulatory process causing regulatory non-linearity (Demmig-Adams et al. 2014, Ruban 2016, van Amerongen and Chmelinov 2020). Sensing constitutive and regulatory dynamics in the time domain may require acclimation to darkness prior to illumination, a protocol that may limit many practically relevant applications in field or greenhouse. With few exceptions (van Kooten et al. 1986, Lebedeva et al. 2002, Lyu and Lazár 2017), interpreting the data by means of mathematical models requires assuming that the rate constants of photosynthetic processes do not change during induction, which contradicts mounting evidence for substantial

conformational changes of photosynthetic proteins during the process (Schansker et al. 2011, Suga et al. 2017, Magyar et al. 2018, Oja and Laisk 2020, Sipka et al. 2021).

To avoid these drawbacks, one can consider studying the dynamic properties of photosynthesis in the frequency-domain by exposing plants and algae to sinusoidally[3] modulated light of a single angular frequency ω. This approach is a valid abstraction of fluctuating light environments appearing in nature due to sun flecks, movement of leaves by wind, shading of leaves by the canopy, or, with phytoplankton, waves on the water surface. From the perspective of mathematical modelling, harmonic modulation is convenient as it appears in Fourier transforms as a single sharp peak, making solution of model differential equations relatively easy (Schwartz 2008). Harmonic oscillations also appear in plant responses to sudden changes in the environment. Laisk and Walker suggested that "understanding oscillations means understanding photosynthesis" (Laisk and Walker 1989). Initially, focus was on spontaneous oscillations induced in plants by, e.g., an abrupt change in the gas phase composition, and measured in Chl fluorescence, oxygen evolution, or CO_2 fixation (Walker et al. 1983, Walker and Sivak 1985, Sivak and Walker 1985, 1986, 1987, Malkin 1987). Several hypotheses have been suggested to explain the spontaneous oscillations (Lazár et al. 2005).

Studying forced oscillations is widely used in physics and engineering. A trivial example can be found in characterizing dielectrics, in which permittivity is measured by scanning over frequencies of a harmonically modulated electric field. This systemic homology is detailed in Supplementary Materials (SM3). The mathematical essentials connected to frequency-domain measurements and analysis are summarized in Supplementary Materials (SM2). Aiming to realize similar potential in photosynthesis research, we propose to complement or, whenever dark adaptation represents a problem, substitute time-domain studies of the dark-to-light transition with frequency-domain measurements of responses to harmonically modulated light.

Scanning over a range of frequencies can address individually dynamically contrasting processes. An additional strength of the proposed frequency-domain investigation is that the measured response can be selectively filtered by hardware or data processing to narrow the sensitivity range close to the forcing frequency of the excitation light (Litovski 2019). Hence, the frequency-domain measurements may provide a higher signal-to-noise ratio than time-domain measurements, which are, by their nature, spread over a broad band of frequencies that are inescapably present in dark-to-light transitions.

[3] We shall henceforth use the general term 'harmonically modulated' rather than the more restrictive term "sinusoidally modulated"

In this work, we present an experimental analysis of Chl fluorescence emission response in green alga *Chlorella sorokiniana* to harmonically modulated light in the range from 1000 to 0.001 Hz. The sub-range 1000 – 1 Hz is characterized for the first time. The observed constitutive non-linearity is investigated using a detailed mathematical model of primary photosynthetic reactions. Implications of the regulatory non-linearity are explored using a simplified, analytically solvable mathematical model of photosynthetic antenna regulation.

The capability of this approach to selectively sense processes within a specific range of rate constants, to sense regulation, and its high signal-to-noise ratio open new opportunities, particularly for broad daytime phenotyping, development of sentinel plants, and stress detection in field and greenhouse, all without a need for dark adaptation.

136

Results

Experiments

Contrasting types of Chl fluorescence yield response to harmonically modulated light measured in a suspension of *Chlorella sorokiniana* are illustrated in Figs. 1A-D. The algae were light-acclimated and the periodic response was largely stationary when measured. The graphs do not start at time 0 to indicate how long the acclimation to oscillating light before the sampling was. Figure 1A depicts the typical Chl fluorescence response to short period (1 s), low-amplitude light modulation (8 - 20%)[4]. Figure 1B depicts dynamics under high-amplitude (8 - 100%, 1 s) modulation. Figures 1C and 1D represent low-amplitude and high-amplitude modulations, respectively, for the longer period of 256 s. Each panel in Fig. 1 consists of two sub-panels with experimental data in the top and numerical analysis in the bottom. The top panels (A1, B1, C1, D1) depict the light modulation (red line) and the measured Chl fluorescence yield response (blue points). The least square fits of the measured data by a combination of up to four sinusoidal functions:

$$Fit(t) = A_0 + A_1 \cdot sin\left[\frac{2\pi(t-\tau_1)}{T}\right] + A_2 \cdot sin\left[\frac{4\pi(t-\tau_2)}{T}\right] + A_3 \cdot sin\left[\frac{6\pi(t-\tau_3)}{T}\right] + A_4 \cdot sin\left[\frac{8\pi(t-\tau_4)}{T}\right]$$

Eq. 1

are represented by thick gray lines in all bottom sub-panels of Fig. 1. The thin lines in panels A2, B2, C2, and D2 represent the individual harmonic components:

- the fundamental harmonics $A_0 + A_1 \cdot sin\left[\frac{2\pi(t-\tau_1)}{T}\right]$ by the thin black line;
- the first upper harmonics $A_0 + A_2 \cdot sin\left[\frac{4\pi(t-\tau_2)}{T}\right]$ by the thin red line;
- the second upper harmonics $A_0 + A_3 \cdot sin\left[\frac{6\pi(t-\tau_3)}{T}\right]$ by the thin green line
- the third upper harmonics $A_0 + A_4 \cdot sin\left[\frac{8\pi(t-\tau_4)}{T}\right]$ by the thin blue line.

[4] The light intensity scale is relative, defined in the instrument protocol in %. The minimum around 8% was found empirically to be the lowest protocol setting with a linear correspondence between protocol and light generated by the instrument. Relationship to the absolute number of PSII turnovers·s^{-1} and absolute light units is described in Materials and Methods.

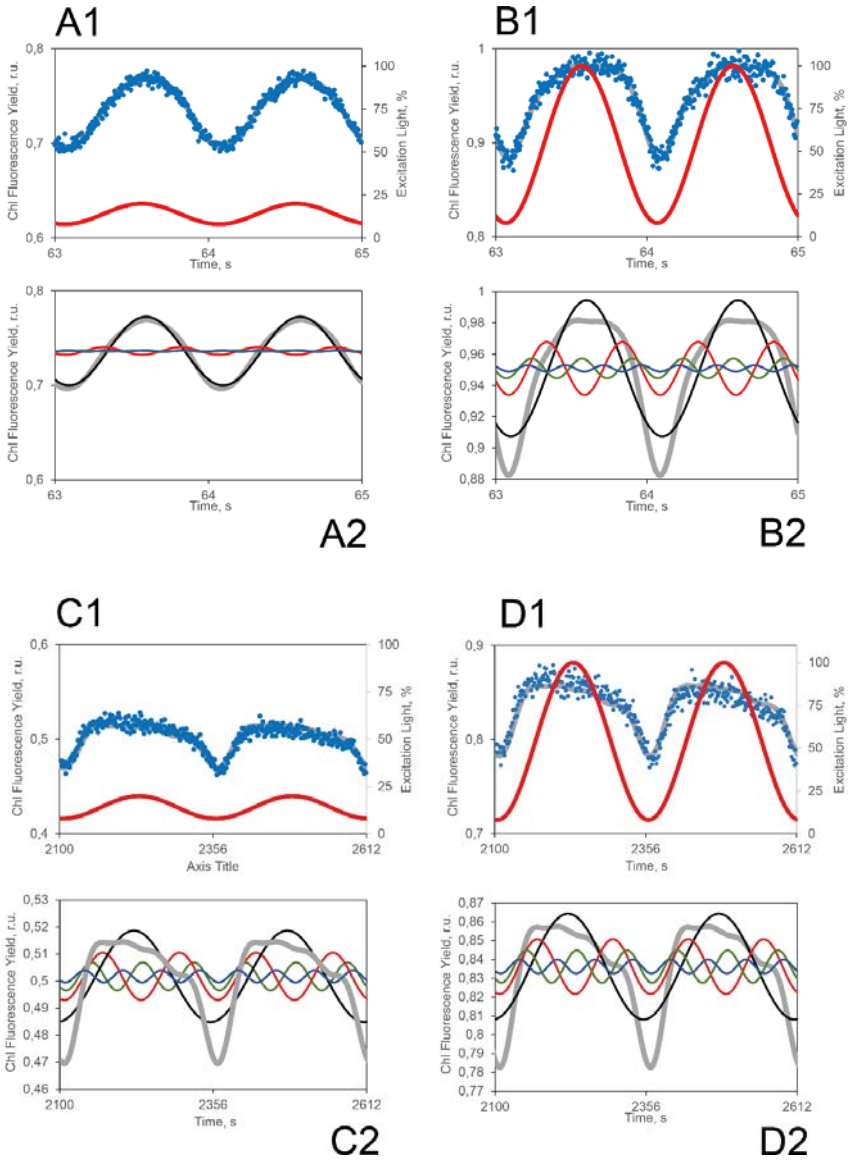

Figure 1. *The thick red lines in panels A1 and B1 show light modulation with a period of 1 second while panels C1 and D1 show a modulation period of 256 seconds. The amplitudes of light oscillations were low in panels A and C (min. 8%, max. 20%) and high (min. 8%, max. 100%) in panels B and D. The corresponding absolute values of photosynthetically active radiation are specified in Materials and Methods. The gray lines in both the top and bottom sub-panels represent numerical fitting of the experimental data by a superposition of one fundamental harmonic component ($\omega = \frac{2\pi}{T}$, thin black line) and up to 3 upper harmonic components: the thin red line with $\omega = 2 \cdot \frac{2\pi}{T}$, the thin green line with $\omega = 3 \cdot \frac{2\pi}{T}$, and the thin blue line with $\omega = 4 \cdot \frac{2\pi}{T}$. The essentials of the numeric analysis are described in detail in Supplementary Materials.*

The response to low-amplitude light oscillating with a period of 1 second (Fig. 1A1) is well fit by the fundamental harmonics, with negligible contributions from upper harmonic modes (Fig. 1A2). Increasing the amplitude of the oscillating light leads to the appearance of an upper harmonic modulation (Fig. 1B1-2) that most likely has, at least to some extent, a trivial explanation by

saturation of photosynthesis around the peak light. Interestingly, the upper harmonic modulation was found in the Ch fluorescence yield response to low-light (Fig. 1C) as well as to high light (Fig. 1D) when the period was 256 seconds. This finding is consistent with earlier reports of upper harmonic modulation occurring with long forcing periods in higher plants and cyanobacteria (Nedbal and Březina 2002, Nedbal et al. 2003, 2005).

Compared to earlier studies, we extend the range of investigated periods in Fig. 2 by at least three orders of magnitude and show the Chl fluorescence yield response for forcing periods between 1 millisecond and 1000 seconds using the same approach and data analysis as in Fig. 1.

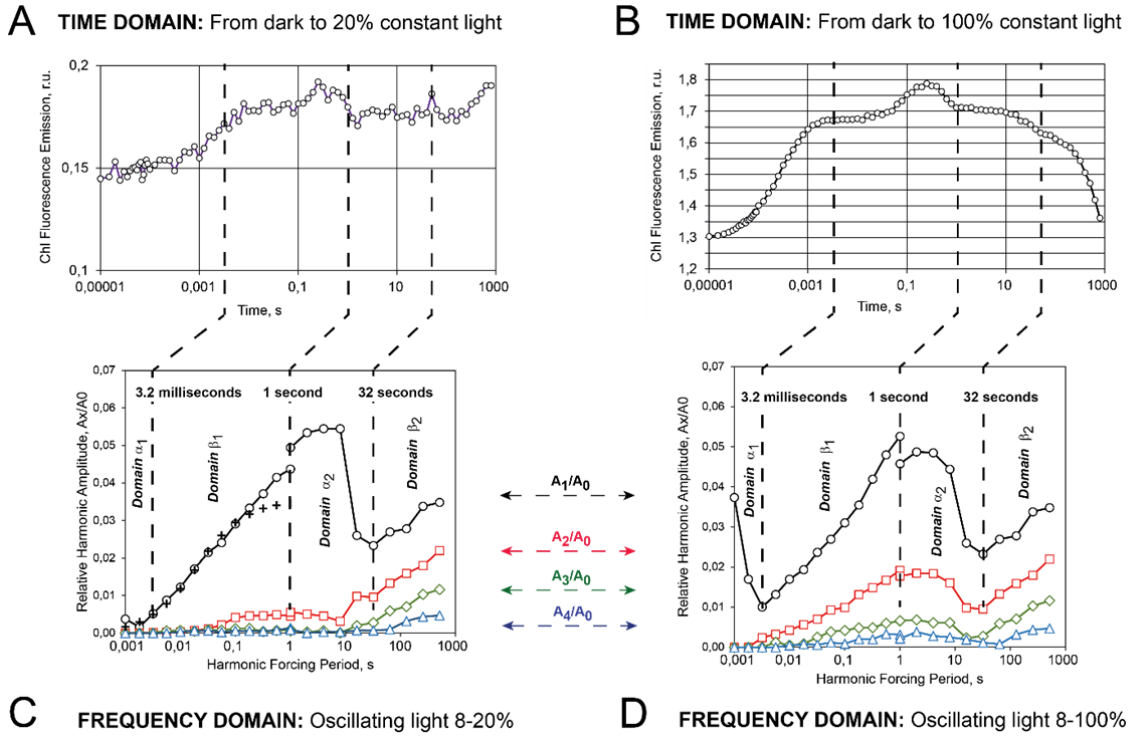

Figure 2. *Comparison of Chl fluorescence dynamics in* C. sorokiniana *measured in response to dark-to-light transition in the time domain (A, B) and in response to harmonically modulated light in the frequency domain (C, D). The color-coding of the fundamental and upper harmonic amplitudes is the same as in Fig. 1 and is also reflected in the legend between panels C and D.*

Figure 2 shows in panels A and B the Chl fluorescence transients measured after exposure of dark-adapted algae to constant light: 20% relative light intensity in panel A and 100% light intensity in panel B. Unlike all other Chl fluorescence measurements reported here, the Chl fluorescence emission shown in Fig. 2 A, B was excited directly by the actinic light and no measuring flashes were used. Identical measurements performed with 20%, 32%, 56% and 100% relative intensity and numerical analysis of the initial photochemical phase of the transients (Lazár et al. 2001) revealed that the light was linearly increasing the photosystem II turnover rate between 20 and 100% in four

equal steps and that 100% relative intensity induced 4930 photosystem II turnovers per second (R^2 = 0.9983). Additional details about effective photosynthetically active irradiance during the measurements are described in Materials and Methods.

The time-domain responses to the dark-to-light transition (Fig. 2A-B) are compared to the frequency responses to harmonically modulated light in panels C and D. The frequency response of photosynthesis by means of Chl fluorescence yield in Fig. 2 can be partitioned into four characteristic frequency domains: α_1 (periods ca. 1 ms - 3.2 ms), β_1 (periods ca. 3.2 ms – 1 s), α_2 (periods ca. 1 s – 32 s), and β_2 (periods ca. 32 s – 512 s). The harmonic components drop with increasing forcing period in domains α_1 and α_2 and increase in domains β_1 and β_2. The increase in the β_1 and β_2 domains is approximately linear in the logarithmic-linear graph in Fig. 2, indicating an exponential relationship in a linear-linear representation.

Heuristic use of the analogy to dielectric permittivity proposed in the Introduction and in Supplementary Materials (SM3-4) as well as considerations proposed in Nedbal and Březina (2002) indicate that the observed frequency dependence might be approximated by $\frac{\beta}{\sqrt{\beta^2+(\omega-\omega_0)^2}}$, where β and ω_0 are empirical parameters and $\omega = \frac{2\pi}{T}$ is the angular frequency of the light modulation. The numerical least-squares fitting in the β_1 domain by $\frac{\beta}{\sqrt{\beta^2+(\omega-\omega_0)^2}}$ is shown in Fig. 2C by black crosses. The quality of the fit is not perfect but the qualitative agreement with experimental data over two orders of magnitude suggests that the dispersion[5] in form common in the theory of dielectric permittivity can be indeed a good heuristic approach.

Another outstanding feature of the frequency response of photosynthesis is the appearance of upper harmonic modes (colored lines in Fig. 2C-D) that appear in two 'waves': the first increasing in the β_1 domain and decreasing in the α_2 domain, and the second monotonically increasing in the β_2 domain. We propose that the upper harmonic modes in β_1, α_2 and those in β_2 are of different molecular origin and use an earlier numerically-solvable model (Lazár 2009) to identify the mechanism of modulation in the β_1, α_2 domains and a new analytically solvable model to show that the upper harmonic modulation in the β_2 domain reflects biological regulation. Both models are graphically represented in Fig. 3.

[5] We adopt the term "dispersion" in the meaning common in the theory of dielectrics, i.e. as a dependence of an observable on the frequency or period of the forcing input, here of harmonically modulated light.

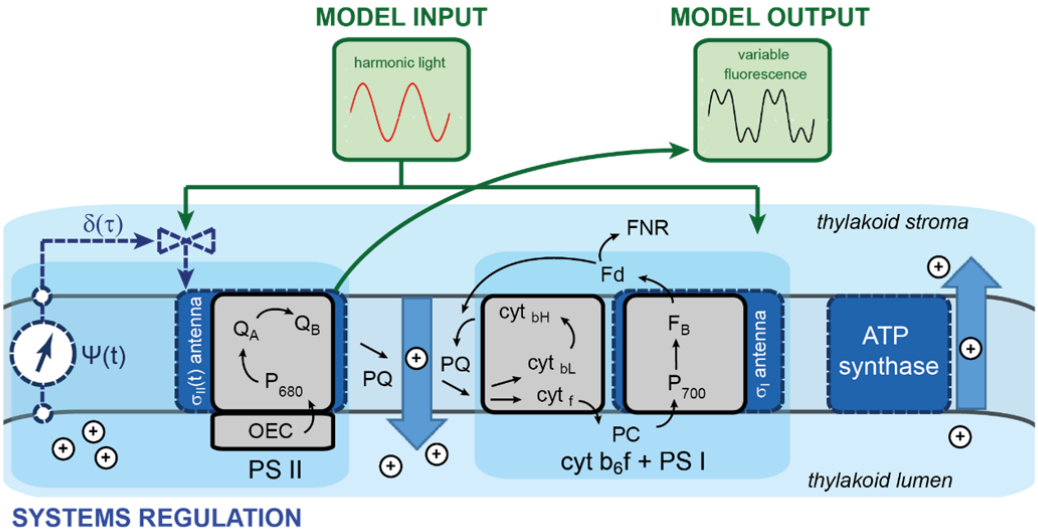

Figure 3. *Simplified graphical representation of the subsystems involved in photosynthesis in an algal thylakoid. The photosynthetic apparatus is exposed to harmonically modulated light (system input* $u(t) = u_0 + u_V \cdot \sin(\omega \cdot t)$*) that drives photochemical reactions in the two photosystems, which are responsible for linear and cyclic electron transport and, eventually, for generation of a difference of the electrochemical potential across the thylakoid membrane. The dynamic response of the system to harmonic forcing is measured by a fluorescence PAM-type sensor. The components considered in the numerically-solvable model (Lazár 2009) are shown in black letters. The blue shaded blocks represent the analytically-solvable model. Complex regulation of photosynthetic reactions is reduced in this scheme to a control of excitation of Photosystem II, which is called non-photochemical quenching (regulation* $\delta(t)$*). More details are explained in the respective parts of the text.*

Numerical solutions of a detailed molecular mathematical model

Detailed molecular models are available for numerical solutions of photosynthetic dynamics during the dark-light transition (Lazár and Schansker 2009, Stirbet et al. 2020) and here we modify the model of Lazár (2009) to additionally explore the dynamics in harmonically modulated light. This model describes electron transport in the thylakoid membrane through Photosystem II, cytochrome b_6/f and Photosystem I to ferredoxin and also cyclic transport (see the components and pathways indicated in Fig. 3 by black letters and arrows). This model was previously used for simultaneous simulation of fast Chl fluorescence induction (the O-J-I-P curve) and of the I_{820} signal that reflects redox state of primary electron donor in Photosystem I, P700, and of electron transporter plastocyanin (Lazár 2009).

The underlying set of differential equations in this model includes a number of non-linear terms that may lead to complex modulation in the Chl fluorescence response, i.e., the exchange of doubly reduced and protonated Q_B with plastoquinone molecules from the pool or electron transport from Photosystem I to ferredoxin. The model also captures saturation of photosynthetic reactions by high light intensities. These phenomena belong to the category of constitutive non-linearities (Bich et al. 2016).

Numerical simulations of forced oscillations of Chl fluorescence yield with a period of 100 ms are shown in Fig. 4, confirming the experimental observations in Fig. 1, namely that forcing by low-amplitude light leads to a variation of Chl fluorescence yield that is very close to a simple sinusoidal function of the forcing period: Fig. 1A for experiment and Fig. 4A for the numerical model. Remaining to be explained by future improved models is the large phase shift between the light and Chl fluorescence response predicted in Fig.4A and not confirmed by the experiment (Fig.1A1).

Substantial deviations from sinusoidal dynamics were observed under strong high-amplitude light modulation (see Fig. 1B (experiment) and Fig. 4B (model)). This deviation was clearly visible in the appearance of upper harmonic modes in the experimentally observed dynamics as well as in the model prediction.

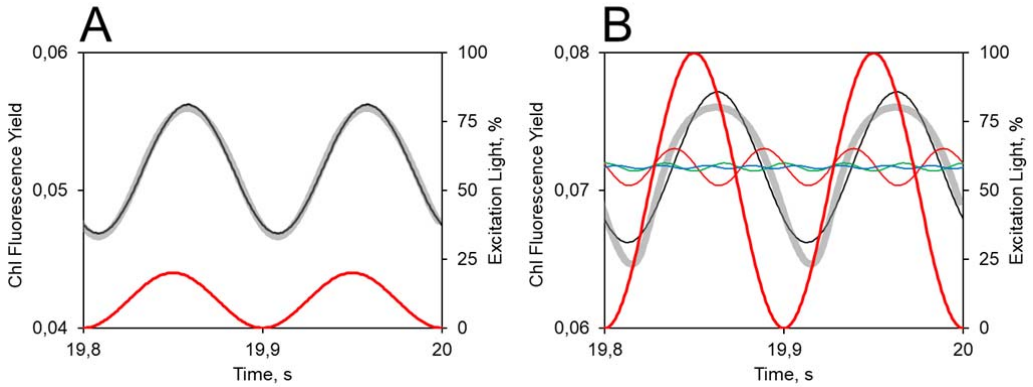

Figure 4. *Modeled Chl fluorescence yield response (thick gray lines) to harmonically modulated light (thick red lines) of low (A) and high amplitude (B). The thin black and colored lines show the result of a least-squares fitting of the modeled dynamics. Color code and fitting functions are the same as in Fig. 1.*

Interestingly, the model predicts that Chl fluorescence modulation amplitude increases with periods increasing from near zero at 1 ms to nearly maximum at 100 s (Fig. 5, black solid line). A rise was also observed experimentally in the β1 domain (3.2 ms - 1 s) (Fig. 2C and green line in Fig.5). However, the model-predicted curve is significantly steeper than the one observed experimentally (Fig. 5, cf. black and green solid lines). Figure 5 also allows comparison of the phase shifts between oscillating light components and Chl fluorescence response predicted by the model (Fig. 5, black dashed line) and observed experimentally (Fig. 5, green dashed line). The model prediction (black dashed line) qualitatively agrees with experiment in trend and amplitude but fails quantitatively and also suggests an inflection in the dispersion that is not seen in the experiment.

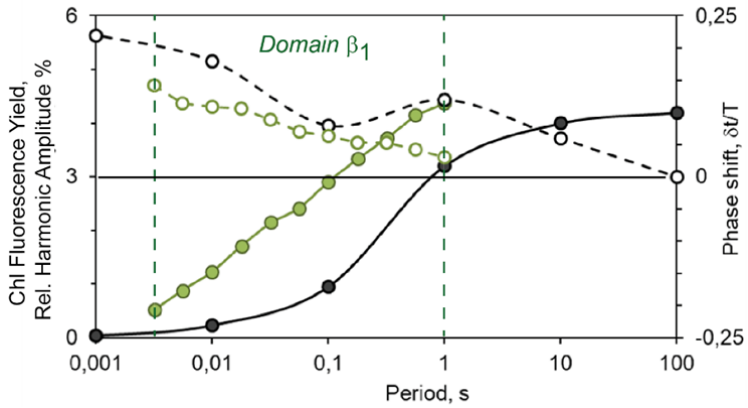

Figure 5. *Comparison of the model-predicted dispersion (see footnote 4 for term explanation) in the amplitude (solid line) and phase (dashed line) of the Chl fluorescence yield response of photosynthetic apparatus to forcing by harmonically modulated light (black lines) with experimental observation (green lines).*

The numerical model is also a potent tool for exploring the dynamics of components not directly observed in the present experiments. A simulated comparison between the closely related Chl fluorescence yield dynamics and plastoquinone redox state is modeled in Fig. 6. Two low-amplitude harmonic light forcing periods were selected for the simulation. The model predicts that light modulation with a period of 0.1 s leads to a simple sinusoidal modulation of Chl fluorescence yield (Fig. 6A), a prediction which agrees with the already presented experimental (Fig. 2) as well as modeling results (Fig. 4). Modulation of the plastoquinone-pool is predicted by the model to be of a very small amplitude (green line in Fig. 6A). This strong damping of plastoquinone redox dynamics is dictated by the size of the plastoquinone pool relative to variations in the in- and outflux of electrons. The large stability of plastoquinone redox state suggested by the green line in Fig. 6A can also indicate that the in- and outflux of electrons in the plastoquinone pool in the short period are largely balanced and synchronized so that the changing light has little effect on the plastoquinone pool redox state. With an increase in the light period to 1 s (Fig. 6B), the fraction of reduced plastoquinone molecules in the pool starts to oscillate strongly and drops sharply around the light minima (green light in Fig. 6B).

The differences between Chl fluorescence dynamics and plastoquinone reduction dynamics (cf. blue and green lines in Fig. 6) underscore the conclusion that measuring the Chl fluorescence signal alone may not be enough to fully elucidate molecular mechanisms that are decisive in a fluctuating light environment. Measurement of additional reporter signals as well as improved mathematical modeling will be necessary to fully understand the dynamics in oscillating light.

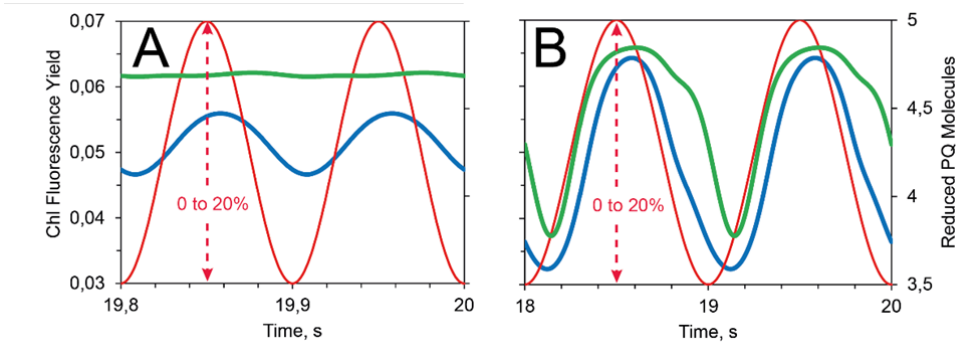

Figure 6. *Dynamics of Chl fluorescence yield (blue) and of reduced plastoquinone molecules (green) predicted for light forcing periods of 0.1 s (A) and 1 s (B), and Photosystem II turnover time corresponding to 20% light in Figs .2A,C. These predictions were generated using the model described in (Lazár 2009). Interesting dynamic details of the plastoquinone reduction in 0.1s modulation (green line in A) are shown in Supplementary Materials (SM1) on an expanded scale.*

Analytical mathematical model

Complex non-linear mathematical models such as the one discussed in the previous paragraphs can only be solved numerically, and a large number of simulations, control analysis, and other advanced mathematical tools are needed for predicting which components contribute to any particular dynamic behavior and by how much. These models are moreover often based on limited knowledge about the true values of the rate constants and most of them assume that the rate constants do not change while the photosynthetic apparatus undergoes induction. These are the deficiencies may explain why agreement between experiment and the detailed model predictions is limited (Fig. 5). This situation by no means delegitimizes the detailed molecular models, rather it suggests that both the detailed bottom-up modeling approaches as well as the top-down approach presented in this section are needed to reflect the different hierarchical levels of the modeled system.

Considering this situation and inspired by the small number and the apparent simplicity of the dynamic features found in the frequency response of photosynthesis (Figs. 1 and 2), we constructed a highly simplified mathematical model of the photosynthetic light reactions that may nevertheless qualitatively simulate this behavior. The essential components of the model are shown in Fig. 3 in blue symbols and letters and, in more detail in Supplementary Materials (SM4).

In a zero-level model approximation, the NPQ regulation of the antenna is assumed to be negligible ($\delta \approx 0$) and the relationship between the electrochemical potential difference across the thylakoid membrane $\Psi_0(t)$ and light $u_0 + u_V \cdot sin(\omega \cdot t)$ (see Fig. SM2) appears as a linear ordinary differential equation:

$$\left(u_0 + u_V \cdot sin(\omega \cdot t)\right) - \alpha \cdot \left(\frac{d\Psi_0(t)}{dt} + \beta \cdot \Psi_0(t)\right) = 0 \qquad \text{Eq. 2}$$

The parameters α and β are shown in the Supplementary Materials (SM4) to depend on the effective size of the photosynthetic antennae, the stoichiometry of coupling between electron and proton

transport, the capacitance of the thylakoid membrane and the rate of ATP-synthesis. Solution of Eq. 2 is derived in detail in Supplementary Materials (SM4). In a stationary limit ($t \gg 1/\beta$) that corresponds to the experiments shown in Fig. 1 and 2, the solution can be expressed as:

$$\Psi_0(t) = \frac{u_0}{\alpha \cdot \beta} + \frac{u_V}{\alpha} \cdot \left[\frac{1}{\sqrt{\beta^2+\omega^2}} \cdot sin\left(\omega \cdot t - arccos\frac{\beta}{\sqrt{\beta^2+\omega^2}}\right)\right] \quad \text{Eq. 3}$$

The model thus predicts that with low-amplitude light modulation and without regulation, $\Psi_0(t)$ will be modulated as a simple sinusoidal function shifted by $arccos\frac{\beta}{\sqrt{\beta^2+\omega^2}}$ in time relative to the light modulation sinus (Eq. 3). No upper harmonic modulation is predicted by the model in the absence of photosynthetic regulation. This prediction qualitatively agrees with the experimental observations in low-light amplitudes and short periods in the domain β_1 shown in Fig. 1A and Fig. 2.

Regulation of Photosystem II antenna size $\delta(\tau)$ approximating NPQ and assumed to be controlled by the electrochemical potential across the thylakoid membrane (Fig. 3), is an example of an interaction that leads to a non-linearity between system output (here Chl fluorescence emission or the electrochemical potential) and light input. This non-linearity originating from regulation contrasts with the previously discussed trivial constitutive non-linearity that occurs due to saturation of the photosynthetic pathways in strong light or due to non-linear primary photosynthetic reactions (Fig. 1B).

With regulation ($\delta > 0$), the equation becomes more complex:

$$u_V \cdot sin(\omega \cdot t) - \alpha \cdot \left(\frac{d\Phi(t)}{dt} + \beta \cdot \Phi(t)\right) = \Delta \cdot \Phi(t) \cdot \left[u_0 \cdot \left(1 - \frac{1}{\alpha\beta}\right) + u_V \cdot sin(\omega \cdot t) - \Phi(t)\right] \quad \text{Eq. 4}$$

, where $\Phi(t)$ is the variable part of the electrochemical potential $\Psi(t)$ and $\Delta = s/2\sigma$ a constant that can, in a specific model, replace the time-variable regulation function *δ(t)* that was introduced in Fig. 3 (for details, see Supplementary Materials, SM4, Eq. SM25a-c). Equation 4 is a first-order ordinary differential equation that is quadratic in the function $\Phi(t)$ and as such belongs to the Riccatti-type of differential equation (Reid 1972). It would be possible to continue with further approximations and iterations towards a more accurate analytical solution but such an effort exceeds the scope and ambition of the present publication. Remarkably, the photosynthetic response to harmonically modulated light can be always deconvolved into a small number of upper harmonic modes, making the dynamics "bumpy", i.e. with clearly discernable shoulders or even local maxima (see also Nedbal and Březina, (2002) for experimental results with higher plants and cyanobacteria). Additionally, the numerical analysis presented in Supplementary Materials (SM2) confirms that the periodic transients can be expected to consist of a small number of upper harmonic modes. Assuming that the regulation is weak ($1 \gg \Delta > 0$), this feature suggests that a solution of Eq. 4 can be sought iteratively in form of a small number of Taylor series terms: $\Psi(t) \approx \Psi_0(t) + \Delta \cdot \Psi_1(t) + \Delta^2 \cdot \Psi_2(t) + \cdots$

As shown in Supplementary Materials (SM4), this approximation can be used to show that the first term in the Taylor series leads to an appearance of the first upper harmonic mode (in bold):

$$\Delta \cdot \Psi_1(t) = \Delta \cdot [A(\omega, \alpha, \beta, u_0, u_v) \cdot sin(\omega \cdot (t - \tau_A(\omega, \alpha, \beta, u_0, u_v)) + \boldsymbol{B(\omega, \alpha, \beta, u_0, u_v)} \cdot \boldsymbol{sin(2 \cdot \omega \cdot (t - \tau_B(\omega, \alpha, \beta, u_0, u_v))}] \quad \text{Eq. 5}$$

The term in Eq. 5 containing the first upper harmonic mode (2ω) proportional to Δ that represents the regulation depicted in Fig. 3. Mathematically, the identical procedure can be used to show that the second and third upper harmonic terms ($3\omega, 4\omega$) appear proportional to Δ^2 and Δ^3. This means that, with a weak regulatory interaction ($1 \gg \Delta > 0$) the upper harmonic modes appear with amplitudes rapidly decreasing with increasing order. The model-supported small number of relevant upper harmonic modes may thus explain the "bumpy" character of the observed photosynthetic response (Nedbal and Březina, (2002) and Figs. 1 and 2).

Equation 4 was derived using multiple crude approximations and additionally the variable part of the electrochemical potential $\Phi(t)$ affects the Chl fluorescence emission only indirectly, by NPQ modulation. The main conclusion is however general: Regulation will introduce in the model differential equations products of light modulation (system input) with system variables ($\Phi(t)$ here or Q_A or PQ pool redox states elsewhere) and squares of systems variables as in Eq. 4. These terms will lead, in the case of harmonic modulation of light, to an appearance of upper harmonic modes in system observables.

345 **Discussion**

346 Forced Chl florescence oscillations, i.e. the Chl fluorescence response to harmonically modulated
347 light, has been so far studied only rarely, with studies in higher plants and cyanobacteria resolving
348 detailed dynamics limited to periods longer than 1 s (Nedbal and Březina 2002, Nedbal et al. 2003,
349 2005, Shimakawa and Miyake 2018, Samson et al. 2019). This study extends the dynamic range to
350 cover nearly 6 orders of magnitude: 1000-0.001 Hz in frequency and 0.001 – 1000 s in periods, and
351 was performed with a green alga.

352 Interestingly, green algae in high-frequency, square modulated light were investigated also earlier by
353 Nedbal et al. (1996) searching for enhancement of photosynthetic rates predicted by the enigmatic
354 flashing light effect (Kok 1953). The conclusion of this early work was that with frequencies
355 approaching 1000 Hz, photosynthesis approached levels that would occur in continuous equivalent
356 light. This was tentatively interpreted as showing that light modulation in this frequency range is
357 integrated by the photosynthetic apparatus. The experiments as well as mathematical model results
358 presented in the present study confirm this earlier hypothesis both experimentally and
359 computationally.

360 The experimental evidence (Figs. 1 and 2) for the dynamic behavior in the domains β_1 (periods 3.2 ms
361 – 1 s), α_2 (periods 1 – 32 s), and β_2 (periods 32 s – 512 s) is strong. However, the discrepancy between
362 model and experiment found in the α_1 domain for periods 1 ms – 3.2 ms (Fig. 2) needs to be re-
363 examined with alternate instrumentation as it was measured at an extreme limit of the present
364 instrument range. With this exception, the data in Fig. 2 are robust and were obtained with different
365 exponentially and late-exponentially growing cultures with little quantitative variability, represented
366 here by the small discontinuity at a period of 1 s. Additionally, the scanning direction was alternating,
367 from short to long periods as well as in the opposite direction. Negative controls were measured with
368 algae that were inactivated by heating to 60 – 80 °C for 10 minutes and, without exception,
369 confirmed absence of any variable Chl fluorescence, confirming that Photosystem II was inactive.
370 Each measuring protocol was also applied to the heat-inactivated samples and the fluorescence yield
371 was confirmed to be independent of any light modulation. In addition to the scanning protocols used
372 to generate the data presented above, measurements were individually performed for each period
373 and amplitude, always with a fresh sample aliquot. Each measurement was repeated three times
374 leading to Bode[6] plots as in Fig. 2. Importantly, two additional intermediate light amplitude
375 modulations were investigated, namely from 8-32% and 8-54% in addition to the 8-20% and 8-100%
376 modulations shown in Figs. 2C and D, respectively. These two additional intermediate light levels

[6] The Bode plot is a graphical representation of frequency dependence of observables that is widely used in control theory.

377 were already strong enough to nearly saturate the photosynthetic pools but did not exhibit the
378 photoinhibitory decline in Chl fluorescence during the long exposure 32 – 1000 s (Fig. 2B). In all other
379 aspects these additional experiments independently confirmed the dynamic behavior in saturating
380 light shown in Fig. 2D.
381 The Bode plots in Fig. 2C and Fig. 5 observed experimentally contrast with the much steeper slopes
382 suggested by the mathematical model (cf. solid green and black lines in Fig. 5). This important
383 qualitative mismatch indicates that models developed for dark-to-light transitions must be amended
384 to correctly describe the dynamic behavior in light-acclimated photosynthetic organisms.
385 Comparison of time-domain (Fig. 2A, B) with frequency-domain measurements (Fig. 2C,D) reveals
386 that the latter can provide information on upper harmonic modes that is unavailable in the
387 conventional PAM time-domain. The information content of the time-domain data can be increased,
388 e.g., by use of saturating pulses, but the same is also possible in the frequency-domain where other
389 dynamic reporters such as the I_{820} signal, CO_2 assimilation rate, non-photochemical quenching and
390 other readouts can be measured (Nedbal et al. 2003).
391 The proposed frequency-domain approach to photosynthetic dynamics and regulation is not only
392 technically advantageous but may contribute to understanding the important phenomena occurring
393 in natural fluctuating day light (Vialet-Cahbrand et al. 2017, Annunziata et al. 2018, Wang et al. 2020)
394 or artificial edge changes in irradiance (Cruz e al. 2016, Adachi et al. 2018, Li et al. 2020). Irradiance
395 fluctuations affect photosynthetic performance and can reveal phenotypes that are not detectable
396 under constant irradiance. Understanding the dynamics of regulation under fluctuating irradiance is
397 essential to improve photosynthetic performance in natural conditions (Rascher and Nedbal 2006,
398 Kaiser et al. 2018, Matsubara 2018, Slattery et al. 2018).
399
400 **Conclusions**
401 Frequency-domain measurements have a high potential for characterizing light-acclimated plants
402 and algae, do not require prior dark adaptation, and are of intrinsically high signal-to-noise ratio. We
403 propose that, as already established in engineering and physics, emancipating the frequency-domain
404 approach in photosynthesis research can release significant potential.
405
406 **Materials and Methods**
407 ***Experimental measurements***
408 *Chlorella sorokiniana* SAG 211-8k was obtained from Göttingen University culture collection and the
409 precultures were inoculated from a Tris-Acetate-Phosphate nutrient medium (TAP) agarose plate and
410 cultivated in TAP medium for 20 h at 30 ˚C in Erlenmeyer flasks (Andersen 2005). The experimental
411 cultures were grown in the same medium but without acetate in a laboratory-build 700 mL column

412 photobioreactor sparged by air. The culture temperature was stabilized at 22°C and irradiance of 200
413 μmol(photons)·m^{-2}· s^{-1} was provided by an array of cold white light emitting diodes. The growth was
414 monitored by measuring optical density in a 1 cm cuvette at 750 nm and the culture was daily diluted
415 for sustained exponential grows. Aliquots of the suspension were sampled and diluted approximately
416 to the optical density 0.3 to 0.5 before the measurements. The measurements of Chl fluorescence
417 emission was performed as described in detail in (Nedbal et al. 2005) using a version of the double-
418 modulation fluorometer (Trtílek et al. 1997) that was custom-modified to generate diverse actinic
419 light patterns. The actinic light of 620 nm was either constant (only in Fig. 2A-B) or harmonically
420 modulated with periods between 1 ms to 512 s (all other experiments). The fidelity of sinusoidal
421 modulation was estimated by numerical fitting of the Chl fluorescence emitted by heat-inactivated
422 algae (10 min. 60 – 80 °C) that was measured without measuring flashes. The deviations from sinus-
423 oidal functions were smaller than 2% when the minimum light intensity during the modulation was
424 8% and above. The scale of light intensity in the measurement cuvette of the instrument was quanti-
425 fied by calculating the numbers of turnovers elicited in Photosystem II per second with 20%, 32%,
426 56%, and 100% relative intensity. The numerical analysis of the initial photochemical phase of the
427 transients (Lazár et al. 2001) revealed that the light was linearly increasing the Photosystem II turno-
428 ver rate between 20 and 100% in four equidistant steps and that 100% relative intensity induced
429 4930 Photosystem II turnovers in a second (R^2 = 0.9983). This number of turnovers is typically
430 reached in higher plants by ca. 5000 μmol(photons)·m^{-2}·s^{-1} (Lazár 2003). With this and considering
431 that the instrument zero, i.e., dark was at about 8% intensity setting, one can estimate effective lev-
432 els of the oscillating light to be:
433 8 – 20% corresponding to oscillations effectively between 0 and 652 μmol(photons)·m^{-2}.s^{-1};
434 8 – 32% to oscillations effectively between 0 and 1304 μmol(photons)·m^{-2}.s^{-1};
435 8 – 56% to oscillations effectively between 0 and 2608 μmol(photons)·m^{-2}.s^{-1};
436 8 – 100% to oscillations effectively between 0 and 5000 μmol(photons)·m^{-2}.s^{-1};
437 The Chl fluorescence dynamics was quantified by relative quantum yield that was measured as Chl
438 fluorescence increment generated by 4.5 μs-long measuring flashes that were added to the harmoni-
439 cally modulated actinic light at defined positions of the period. The stability of the measuring flashes
440 on the background of harmonically modulated actinic light was another instrument feature that was
441 checked to avoid artifacts. We assessed this stability by measuring, for each protocol setting and for
442 each period of modulation, Chl fluorescence elicited by the flash in heat-inactivated algae that exhib-
443 ited no change in yield over the measuring period. The stability was better than 1%.
444 The experimental protocols were using 200 measuring flashes per actinic light period, only with the
445 shortest periods 1-10 ms, the number of flashes per period was reduced to 100.

Two types of protocols were used to demonstrate that the measurement results were independent of the protocol. The first type was designed to probe response with a particular period of harmonic light forcing T. It started with induction achieved by 60 periods T_{ind}=1s of actinic light. The Chl fluorescence response to a particular selected angular frequency $\omega = \frac{2\pi}{T}$ was then probed by applying 5 or 10 periods T. Only the last three periods were considered approximately stationary and used for further numerical analysis that was done by least-square fitting by Solver in Microsoft Excel.

The second protocol type was designed for scanning over many light modulation periods and was used in two variants: The first protocol variant was starting with induction by 100 periods of T_{ind}=1s of actinic light that were followed by ten measuring periods, each of T = 1000, 562, 316, 178, 100, 56, 32, 18, 10, 5.6, 3.2, 1.8 and 1 ms. The second protocol variant was also starting with induction by 100 periods of T_{ind}=1s of actinic light, followed by five measuring periods for T = 1, 2, 4, 8, 16, 32, 64, 128, 256, and 512 s.

Numerically Solved Model

The numerically solved model used in this work is the model originally published in Lazár (2009). Original goal for construction of the model was to show, by means of mathematical simulations, that electron transport in and beyond photosystem II shapes decisively the O-J-I-P Chl fluorescence transient. The argument required parallel measurement of I_{820} transmission signal. Transmission at 820 nm is modulated by the redox state of primary electron donor in photosystem I (P700), and plastocyanin.

To describe this, the model had to consider the electron transport including: photosystem II with oxygen evolving complex, cytochrome b_6/f and photosystem I protein complexes, plastoquinone pool in the thylakoid membrane, plastocyanin in lumen and ferredoxin and ferredoxin-NADPH-oxidoreductase in stroma (see Fig. 3). Function of particular complexes is described by redox reactions between the four S-states (S_0, S_1, S_2, S_3) for oxygen evolving complex, between the primary electron donor, P680, and the first and the second quinone electron acceptors, Q_A and Q_B, respectively, for Photosystem II, between heme f, low and high potential hemes b, and heme c for cytochrome b_6/f, and between primary electron donor, P700, and iron-sulfur center F_B, for photosystem I. Since the electron donors and acceptors are fixed in the proteins, electron transport between them is described by the first order kinetics where each redox state of a protein represents combination of redox states of its electron carriers. For example, the initial redox state of photosystem II is described as $P680Q_AQ_B$, which is transformed to $P680^+Q_A^-Q_B$ due to the charge separation caused by absorption of light. Thus, photosystem II has 2 (P680, $P680^+$) x 2 (Q_A, Q_A^-) x 3 (Q_B, Q_B^-, Q_B^{2-}) = 12 states, time evolution of each of them being described by a differential equation.

Similarly, cytochrome b_6/f has 12 states, and photosystem I 4 states. Electron transport to/from plastoquinone pool, plastocyanin and ferredoxin is described by the second order kinetics. Not to complicate photosystem II description by additional multiplication number of its states by 4 (for 4 S-states of oxygen evolving complex), electron transport during the S-states transition to $P680^+$ is described by the second order kinetics. Ferredoxin-NAPDH oxidoreductase is initially oxidized and inactive and after its activation it is consequently reduced twice by electrons from ferredoxin and the turnover of doubly reduced Ferredoxin-NAPDH oxidoreductase to active oxidized Ferredoxin-NAPDH oxidoreductase (the first order kinetics) reflects NADPH formation. To be able to simulate the Chl fluorescence data in agreement with the experiments, cyclic electron transport from ferredoxin directly to plastoquinone pool was considered (see Fig. 3), described by third order kinetics (electrons from two reduced ferredoxin molecules are necessary to reduce one plastoquinone molecule). Altogether, the model is a set of 42 ordinary differential equations, which was solved numerically in Matlab (MathWorks, USA). The oscillating excitation light enters the model in time-dependent value of rate constants of charge separation in photosystem II and photosystem I, i.e., in reaction $P680Q_AQ_B^{(-,2-)}$ -> $P680^+Q_A^-Q_B^{(-,2-)}$ for photosystem II and in reaction $P700F_B$ -> $P700^+F_B^-$ for photosystem I. The rate constants equal to $k_{max} \times 0.5 \times (1 - \cos(2 \times \pi \times t/T))$, where k_{max} is maximal value of the rate constant (equal to 100 or 500 s^{-1} for simulations in Figs. 4A and 6 and in Fig. 4B, respectively), which is proportional to intensity of excitation light (100% intensity ≈ k_{max} = 500 s^{-1}), and T is period of the oscillations (equal to 0.1 s for simulations in Figs. 4A, 4B, and 6A, and 1 s in Fig, 6B, respectively), and t is time. Values of the other rate constants and initial conditions were taken from the literature (see Lazár 2009). Quantum yield of Chl fluorescence, which is shown in Figs. 4 and 6 and to which the experimentally measured Chl fluorescence signal was proportional, was defined as $\Phi_F(t) = \Phi_0 \times \Sigma Q_A(t) + \Phi_M \times \Sigma Q_A^-(t)$, where Φ_0 (= 0.02) and Φ_M (= 0.08, Lazár 1999) are quantum yields of Chl fluorescence when Photosystem II reaction centers are open (i.e., with Q_A) or closed (i.e., with Q_A^-), respectively and $\Sigma Q_A(t)$ and $\Sigma Q_A^-(t)$ are sums of all photosystem II states with Q_A and Q_A^-, respectively.

Acknowledgements

In addition to the acknowledgements to funding agencies stated elsewhere, the authors appreciate critical reading and feedback of Silvia Schrey, Shizue Matsubara, and Steven (Dean) Calahan from Forschungszentrum Jülich in Germany, Jakub Nedbal from King's College London in UK, and Johan Grobbelaar from University of Orange Free State, S.Africa. Validation of our mathematical derivations was done by Antonín Slavík from Faculty of Mathematics and Physics, Charles University Prague, Czech Republic. Language was thoroughly edited by Steven (Dean) Calahan.

515

Parsed Citations

Debye P. (1913) Ver. Deut. Phys. Gesell. 15, 777
Google Scholar: Author Only Title Only Author and Title

James F.A.J.L., ed. (1996) The Correspondence of Micheal Faraday, Volume 3, 1841-1848, Letter 1674, pp. 317-318. The Institution of Electrical Engineering and Technology, London, United Kingdom
Google Scholar: Author Only Title Only Author and Title

Lazár D. (2009) Modelling of light-induced chlorophyll a fluorescence rise (O-J-I-P transient) and changes in 820 nm-transmittance signal of photosynthesis. Photosynthetica 47, 483-498
Google Scholar: Author Only Title Only Author and Title

Nedbal L., Březina V. (2002) Complex metabolic oscillations in plants forced by harmonic irradiance. Biophysical Journal 83, 2180-2189
Google Scholar: Author Only Title Only Author and Title

Nedbal L., Březina V., Adamec F., Štys D., Oja V, Laisk A., Govindjee (2003) Negative feedback regulation is responsible for the non-linear modulation of photosynthetic activity in plants and cyanobacteria exposed to a dynamic light environment. Biochimica et Biophysica Acta -Bioenergetics 1607, 5-17
Google Scholar: Author Only Title Only Author and Title

Nedbal L., Březina V., Červený J., Trtílek M. (2005) Photosynthesis in dynamic light: systems biology of unconventional chlorophyll fluorescence transients in Synechocystis sp. PCC 6803. Photosynthesis Research 84, 99-106
Google Scholar: Author Only Title Only Author and Title

Schwartz L. (2008) Mathematics for the physical sciences. Courier Dover Publications
Google Scholar: Author Only Title Only Author and Title

von Bertalanffy L. (1993) General system theory: Foundations, development, applications. Georges Braziller, Inc., 1993.
Google Scholar: Author Only Title Only Author and Title

Debye P. (1913) Ver. Deut. Phys. Gesell. 15, 777
Google Scholar: Author Only Title Only Author and Title

James F.A.J.L., ed. (1996) The Correspondence of Micheal Faraday, Volume 3, 1841-1848, Letter 1674, pp. 317-318. The Institution of Electrical Engineering and Technology, London, United Kingdom
Google Scholar: Author Only Title Only Author and Title

Lazár D. (2009) Modelling of light-induced chlorophyll a fluorescence rise (O-J-I-P transient) and changes in 820 nm-transmittance signal of photosynthesis. Photosynthetica 47, 483-498
Google Scholar: Author Only Title Only Author and Title

Nedbal L., Březina V. (2002) Complex metabolic oscillations in plants forced by harmonic irradiance. Biophysical Journal 83, 2180-2189
Google Scholar: Author Only Title Only Author and Title

Nedbal L., Březina V., Adamec F., Štys D., Oja V, Laisk A., Govindjee (2003) Negative feedback regulation is responsible for the non-linear modulation of photosynthetic activity in plants and cyanobacteria exposed to a dynamic light environment. Biochimica et Biophysica Acta -Bioenergetics 1607, 5-17
Google Scholar: Author Only Title Only Author and Title

Nedbal L., Březina V., Červený J., Trtílek M. (2005) Photosynthesis in dynamic light: systems biology of unconventional chlorophyll fluorescence transients in Synechocystis sp. PCC 6803. Photosynthesis Research 84, 99-106
Google Scholar: Author Only Title Only Author and Title

Schwartz L. (2008) Mathematics for the physical sciences. Courier Dover Publications
Google Scholar: Author Only Title Only Author and Title

von Bertalanffy L. (1993) General system theory: Foundations, development, applications. Georges Braziller, Inc., 1993.
Google Scholar: Author Only Title Only Author and Title

Debye P. (1913) Ver. Deut. Phys. Gesell. 15, 777
Google Scholar: Author Only Title Only Author and Title

James F.A.J.L., ed. (1996) The Correspondence of Micheal Faraday, Volume 3, 1841-1848, Letter 1674, pp. 317-318. The Institution of Electrical Engineering and Technology, London, United Kingdom
Google Scholar: Author Only Title Only Author and Title

Lazár D. (2009) Modelling of light-induced chlorophyll a fluorescence rise (O-J-I-P transient) and changes in 820 nm-transmittance signal of photosynthesis. Photosynthetica 47, 483-498
Google Scholar: Author Only Title Only Author and Title

Nedbal L., Březina V. (2002) Complex metabolic oscillations in plants forced by harmonic irradiance. Biophysical Journal 83, 2180-2189
Google Scholar: Author Only Title Only Author and Title

Nedbal L., Březina V., Adamec F., Štys D., Oja V, Laisk A., Govindjee (2003) Negative feedback regulation is responsible for the non-linear modulation of photosynthetic activity in plants and cyanobacteria exposed to a dynamic light environment. Biochimica et Biophysica Acta -Bioenergetics 1607, 5-17
Google Scholar: Author Only Title Only Author and Title

Nedbal L., Březina V., Červený J., Trtílek M. (2005) Photosynthesis in dynamic light: systems biology of unconventional chlorophyll fluorescence transients in Synechocystis sp. PCC 6803. Photosynthesis Research 84, 99-106
Google Scholar: Author Only Title Only Author and Title

Schwartz L. (2008) Mathematics for the physical sciences. Courier Dover Publications
Google Scholar: Author Only Title Only Author and Title

von Bertalanffy L. (1993) General system theory: Foundations, development, applications. Georges Braziller, Inc., 1993.
Google Scholar: Author Only Title Only Author and Title